

Supplemental Material for Surface instability in nodal noncentrosymmetric superconductors

Carsten Timm, Stefan Rex, and P. M. R. Brydon

I. MEAN-FIELD THEORY FOR THE BULK

In this section we sketch the MF theory for the bulk NCS. We assume spatially uniform pairing potentials $\Delta_j^s = \Delta_s$ and $\Delta_{ij}^t = \Delta_t$. Using this ansatz to decouple the interaction Hamiltonian H_{int} , we obtain the Bogoliubov-de Gennes (BdG) Hamiltonian [S1]

$$H_{\text{MF}} = \frac{1}{2} \sum_{\mathbf{k}} \Phi_{\mathbf{k}}^\dagger \mathcal{H}(\mathbf{k}) \Phi_{\mathbf{k}} + N \frac{\Delta_s^2}{U_s} + N \frac{\Delta_t^2}{U_t}, \quad (\text{S1})$$

with the number of sites, N , and the block matrix

$$\mathcal{H}(\mathbf{k}) = \begin{pmatrix} h(\mathbf{k}) & \Delta(\mathbf{k}) \\ \Delta^\dagger(\mathbf{k}) & -h^T(-\mathbf{k}) \end{pmatrix} \quad (\text{S2})$$

written in terms of $h(\mathbf{k}) = \xi_{\mathbf{k}} \sigma^0 - \lambda \mathbf{l}_{\mathbf{k}} \cdot \boldsymbol{\sigma}$, $\Delta(\mathbf{k}) = (\Delta_s \sigma^0 + \Delta_t \mathbf{l}_{\mathbf{k}} \cdot \boldsymbol{\sigma}) i \sigma^y$, $\xi_{\mathbf{k}} = -2t (\cos k_x + \cos k_y + \cos k_z) - \mu$, $\mathbf{l}_{\mathbf{k}} = \hat{\mathbf{x}} \sin k_y - \hat{\mathbf{y}} \sin k_x$, and the Nambu spinor $\Phi_{\mathbf{k}} = (c_{\mathbf{k}\uparrow}, c_{\mathbf{k}\downarrow}, c_{-\mathbf{k},\uparrow}^\dagger, c_{-\mathbf{k},\downarrow}^\dagger)^T$. Here, σ^0 is the 2×2 identity matrix. The dispersion $E_{\mathbf{k}\nu}$, $\nu = 1, \dots, 4$ is obtained by diagonalizing $\mathcal{H}(\mathbf{k})$. Δ_s and Δ_t are then obtained by minimizing the free energy

$$F_{\text{MF}} = -k_B T \sum'_{\mathbf{k}\nu} \ln \left(2 \cosh \frac{\beta E_{\mathbf{k}\nu}}{2} \right) + N \frac{\Delta_s^2}{U_s} + N \frac{\Delta_t^2}{U_t}, \quad (\text{S3})$$

where the momentum sum is over half the BZ, $k_m > 0$. This restriction of the sum makes use of particle-hole symmetry, which relates the Hamiltonian in Eq. (S2) at \mathbf{k} and $-\mathbf{k}$ by [S1] $\mathcal{U}_C \mathcal{H}^T(-\mathbf{k}) \mathcal{U}_C^\dagger = -\mathcal{H}(\mathbf{k})$ with the unitary matrix $\mathcal{U}_C = \sigma^x \otimes \sigma^0$.

II. MEAN-FIELD THEORY FOR THE SLAB

We now set up the MF Hamiltonian for the (101) slab and describe the determination of the gap parameters Δ_l^s , $\Delta_{l+1/2}^x$, and Δ_l^y in the MF approximation. After Fourier transformation in the directions parallel to the surfaces, the MF Hamiltonian reads

$$H_{\text{MF}} = \frac{1}{2} \sum_{\mathbf{k}} \sum_{l=0}^{W-1} \Phi_{\mathbf{k}l}^\dagger \mathcal{H}_{ll}(\mathbf{k}) \Phi_{\mathbf{k}l} + \frac{1}{2} \sum_{\mathbf{k}} \sum_{l=0}^{W-2} \Phi_{\mathbf{k},l+1}^\dagger \mathcal{H}_{l+1,l}(\mathbf{k}) \Phi_{\mathbf{k}l} + \frac{1}{2} \sum_{\mathbf{k}} \sum_{l=1}^{W-1} \Phi_{\mathbf{k},l-1}^\dagger \mathcal{H}_{l-1,l}(\mathbf{k}) \Phi_{\mathbf{k}l} \\ + \frac{N_{\parallel}}{U_s} \sum_{l=0}^{W-1} |\Delta_l^s|^2 + \frac{N_{\parallel}}{2U_t} \sum_{l=0}^{W-2} |\Delta_{l+1/2}^x|^2 + \frac{N_{\parallel}}{2U_t} \sum_{l=0}^{W-1} |\Delta_l^y|^2, \quad (\text{S4})$$

where N_{\parallel} is the number of unit cells of the slab and $\Phi_{\mathbf{k}l} = (c_{\mathbf{k}l\uparrow}, c_{\mathbf{k}l\downarrow}, c_{-\mathbf{k},l,\uparrow}^\dagger, c_{-\mathbf{k},l,\downarrow}^\dagger)^T$ is the partially Fourier-transformed Nambu spinor. The sums over l containing $\Phi_{\mathbf{k},l\pm 1}^\dagger$ are restricted in such a way that $l \pm 1 \in \{0, \dots, W-1\}$. The coefficient matrices appearing in H_{MF} are

$$\mathcal{H}_{ll}(\mathbf{k}) = \begin{pmatrix} -2t \cos k_y - \mu & -\lambda \sin k_y & -\Delta_l^y \sin k_y & \Delta_l^s \\ -\lambda \sin k_y & -2t \cos k_y - \mu & -\Delta_l^s & \Delta_l^y \sin k_y \\ -\Delta_l^{y*} \sin k_y & -\Delta_l^{s*} & 2t \cos k_y + \mu & -\lambda \sin k_y \\ \Delta_l^{s*} & \Delta_l^{y*} \sin k_y & -\lambda \sin k_y & 2t \cos k_y + \mu \end{pmatrix}, \quad (\text{S5})$$

$$\mathcal{H}_{l\pm 1,l}(\mathbf{k}) = \begin{pmatrix} -2t \cos(k_m/\sqrt{2}) & \pm(\lambda/2) e^{\mp i k_m/\sqrt{2}} & \pm(\Delta_{l\pm 1/2}^x/2) e^{\mp i k_m/\sqrt{2}} & 0 \\ \mp(\lambda/2) e^{\mp i k_m/\sqrt{2}} & -2t \cos(k_m/\sqrt{2}) & 0 & \pm(\Delta_{l\pm 1/2}^x/2) e^{\mp i k_m/\sqrt{2}} \\ \mp(\Delta_{l\pm 1/2}^{x*}/2) e^{\mp i k_m/\sqrt{2}} & 0 & 2t \cos(k_m/\sqrt{2}) & \mp(\lambda/2) e^{\mp i k_m/\sqrt{2}} \\ 0 & \mp(\Delta_{l\pm 1/2}^{x*}/2) e^{\mp i k_m/\sqrt{2}} & \pm(\lambda/2) e^{\mp i k_m/\sqrt{2}} & 2t \cos(k_m/\sqrt{2}) \end{pmatrix}. \quad (\text{S6})$$

We next construct the $4W \times 4W$ block matrix

$$\mathcal{H}(\mathbf{k}) \equiv \begin{pmatrix} \mathcal{H}_{00}(\mathbf{k}) & \mathcal{H}_{01}(\mathbf{k}) & 0 & \cdots \\ \mathcal{H}_{10}(\mathbf{k}) & \mathcal{H}_{11}(\mathbf{k}) & \mathcal{H}_{12}(\mathbf{k}) & \cdots \\ 0 & \mathcal{H}_{21}(\mathbf{k}) & \mathcal{H}_{22}(\mathbf{k}) & \cdots \\ \vdots & \vdots & \vdots & \ddots \end{pmatrix} \quad (\text{S7})$$

and denote its eigenvalues by $E_{\mathbf{k}\nu}$, $\nu = 1, \dots, 4W$ and the corresponding eigenvectors by $|\mathbf{k}\nu\rangle$. The MF Hamiltonian satisfies particle-hole symmetry [S1], $\mathcal{U}_C \mathcal{H}^T(-\mathbf{k}) \mathcal{U}_C^\dagger = -\mathcal{H}(\mathbf{k})$ with the unitary matrix $\mathcal{U}_C = \mathbb{1}_W \otimes \sigma^x \otimes \sigma^0$, where $\mathbb{1}_W$ is the $W \times W$ identity matrix. This symmetry again allows to restrict the momentum sums to half the BZ. The free energy can then be written as

$$F_{\text{MF}} = -k_B T \sum'_{\mathbf{k}\nu} \ln \left(2 \cosh \frac{\beta E_{\mathbf{k}\nu}}{2} \right) + \frac{N_{\parallel}}{U_s} \sum_{l=0}^{W-1} |\Delta_l^s|^2 + \frac{N_{\parallel}}{2U_t} \sum_{l=0}^{W-2} |\Delta_{l+1/2}^x|^2 + \frac{N_{\parallel}}{2U_t} \sum_{l=0}^{W-1} |\Delta_l^y|^2, \quad (\text{S8})$$

where the momentum sum is restricted to half the BZ, $k_m > 0$. Minimization of F_{MF} gives the gaps Δ_l^s , $\Delta_{l+1/2}^x$, and Δ_l^y . The derivatives of F_{MF} with respect to the complex conjugate gaps can be calculated with the help of the Hellmann-Feynman theorem, for example

$$\frac{\partial F_{\text{MF}}}{\partial \Delta_l^{s*}} = -\frac{1}{2} \sum'_{\mathbf{k}\nu} \tanh \frac{\beta E_{\mathbf{k}\nu}}{2} \langle \mathbf{k}\nu | \frac{\partial \mathcal{H}(\mathbf{k})}{\partial \Delta_l^{s*}} | \mathbf{k}\nu \rangle + \frac{N_{\parallel}}{U_s} \Delta_l^s. \quad (\text{S9})$$

The momentum sums are performed on a 50×50 mesh, referring to the full surface BZ. Quadrupling the number of points in the mesh to 100×100 leads to changes in the MF gaps on the order of only 0.1%.

Solving the resulting MF equations by iteration turns out to be prohibitively slow for the required W , essentially because the minimum of F_{MF} is very shallow in some directions in the high-dimensional space of gap parameters. On the other hand, numerical minimization making use of the explicitly known gradient is reasonably efficient. We use the Broyden-Fletcher-Goldfarb-Shanno method implemented in Numerical Recipes [S2]. It requires an initial guess for the inverse Hessian. When we scan over ranges of temperatures, we use not only the converged values of the gaps but also the best approximate inverse Hessian from one step as starting values for the next, which significantly speeds up the convergence. We assume that the method has converged when no real or imaginary part of any gap parameter changes by more than (double) machine precision in the last step.

For certain parameter values, we find nonvanishing gradients of the phases of the order parameters in the l direction, normal to the surfaces. Specifically, we find four metastable solutions, which are mapped onto each other by inverting the phase gradients at one or both surfaces. In the limit $W \rightarrow \infty$, the four solutions are degenerate. For finite W , they split into two degenerate pairs with phase gradients that are even and odd, respectively, under reflection at the center of the slab. We here choose a solution with even phase gradients since then the self-consistent solution ensures that the phases of Δ_l^s , $\Delta_{l+1/2}^x$, and Δ_l^y become equal at the center of the slab; equal phases of all gaps at the center are expected since the bulk MF solution has equal phases. By a global phase change we can then make the phase of all gaps zero at the center. The phases and imaginary parts of the gaps are then odd under reflection at the center. Finally, of the two remaining solutions differing in the sign of the imaginary parts of the gaps, we select the solution with $\text{Im} \Delta_0^s \geq 0$ for definiteness. The other solution leads to inverted spin polarizations and currents.

III. SPIN POLARIZATION

Here, we present expressions for the spin polarization. The operator of the spin per site, averaged over the directions parallel to the surfaces, is

$$\mathbf{s}_l = \frac{1}{N_{\parallel}} \sum_{\mathbf{k}} c_{\mathbf{k}l}^\dagger \frac{\boldsymbol{\sigma}}{2} c_{\mathbf{k}l}. \quad (\text{S10})$$

Using particle-hole symmetry, the thermal spin average can be written as

$$\langle \mathbf{s}_l \rangle = -\frac{1}{4N_{\parallel}} \sum'_{\mathbf{k}\nu} \tanh \frac{\beta E_{\mathbf{k}\nu}}{2} \langle \mathbf{k}\nu | P_{ll} \otimes \begin{pmatrix} \boldsymbol{\sigma} & 0 \\ 0 & -\boldsymbol{\sigma}^T \end{pmatrix} | \mathbf{k}\nu \rangle, \quad (\text{S11})$$

where $P_{ll'}$ is a $W \times W$ matrix with the components $(P_{ll'})_{nn'} = \delta_{ln} \delta_{l'n'}$. We also consider the momentum-dependent contributions to the spin polarization of the half slab defined by $0 \leq l < W/2$. These contributions are obtained by summing $\langle \mathbf{s}_l \rangle$ over $l = 0, \dots, W/2 - 1$ and removing the factor $1/N_{\parallel}$ and the momentum sum.

IV. EQUILIBRIUM CURRENT

The second observable of interest is the current. The operators j_{ij}^α denote the *electron-number* current from site j to its nearest neighbor i in the $\alpha = x, y, z$ direction. They can be read off from H_0 in Eq. (1) in the main text,

$$j_{ij}^x = -i c_i^\dagger \begin{pmatrix} -t & \lambda/2 \\ -\lambda/2 & -t \end{pmatrix} c_j + i c_j^\dagger \begin{pmatrix} -t & -\lambda/2 \\ \lambda/2 & -t \end{pmatrix} c_i, \quad (\text{S12})$$

$$j_{ij}^y = -i c_i^\dagger \begin{pmatrix} -t & -i\lambda/2 \\ -i\lambda/2 & -t \end{pmatrix} c_j + i c_j^\dagger \begin{pmatrix} -t & i\lambda/2 \\ i\lambda/2 & -t \end{pmatrix} c_i, \quad (\text{S13})$$

$$j_{ij}^z = -i c_i^\dagger \begin{pmatrix} -t & 0 \\ 0 & -t \end{pmatrix} c_j + i c_j^\dagger \begin{pmatrix} -t & 0 \\ 0 & -t \end{pmatrix} c_i. \quad (\text{S14})$$

The interaction term H_{int} conserves charge locally and therefore does not contribute to the current operator. After the MF decoupling, the anomalous terms do not conserve charge—they describe creation or annihilation of two electrons either at the same site or at neighboring sites. Such processes do not lead to currents but do introduce a source term, which is discussed in the main text. We average the current over layers parallel to the surface, taking into account that j_{ij}^x and j_{ij}^z connect adjacent layers, whereas j_{ij}^y describes a current within a single layer. We then obtain the thermal averages, again using particle-hole symmetry,

$$\langle j_{l+1/2}^x \rangle = -\frac{1}{2N_\parallel} \sum'_{\mathbf{k}\nu} \tanh \frac{\beta E_{\mathbf{k}\nu}}{2} \langle \mathbf{k}\nu | \left\{ i e^{-ik_m/\sqrt{2}} P_{l+1,l} \otimes \begin{pmatrix} t & -\lambda/2 & 0 & 0 \\ \lambda/2 & t & 0 & 0 \\ 0 & 0 & t & -\lambda/2 \\ 0 & 0 & \lambda/2 & t \end{pmatrix} + \text{H.c.} \right\} | \mathbf{k}\nu \rangle, \quad (\text{S15})$$

$$\langle j_l^y \rangle = -\frac{1}{N_\parallel} \sum'_{\mathbf{k}\nu} \tanh \frac{\beta E_{\mathbf{k}\nu}}{2} \langle \mathbf{k}\nu | P_{ll} \otimes \begin{pmatrix} t \sin k_y & -(\lambda/2) \cos k_y & 0 & 0 \\ -(\lambda/2) \cos k_y & t \sin k_y & 0 & 0 \\ 0 & 0 & t \sin k_y & (\lambda/2) \cos k_y \\ 0 & 0 & (\lambda/2) \cos k_y & t \sin k_y \end{pmatrix} | \mathbf{k}\nu \rangle, \quad (\text{S16})$$

$$\langle j_{l+1/2}^z \rangle = -\frac{1}{2N_\parallel} \sum'_{\mathbf{k}\nu} \tanh \frac{\beta E_{\mathbf{k}\nu}}{2} \langle \mathbf{k}\nu | \left\{ i e^{ik_m/\sqrt{2}} P_{l+1,l} \otimes \begin{pmatrix} t & 0 & 0 & 0 \\ 0 & t & 0 & 0 \\ 0 & 0 & t & 0 \\ 0 & 0 & 0 & t \end{pmatrix} + \text{H.c.} \right\} | \mathbf{k}\nu \rangle, \quad (\text{S17})$$

where $\langle j_{l+1/2}^{x,z} \rangle$ denotes currents connecting layers l and $l+1$. The components with respect to the slab coordinates are

$$\langle j_{l+1/2}^l \rangle = \frac{\langle j_{l+1/2}^x \rangle + \langle j_{l+1/2}^z \rangle}{\sqrt{2}}, \quad \langle j_{l+1/2}^m \rangle = \frac{\langle j_{l+1/2}^x \rangle - \langle j_{l+1/2}^z \rangle}{\sqrt{2}}. \quad (\text{S18})$$

We note that $\langle j_l^y \rangle$ vanishes for any choice of gap parameters for our model, even non-selfconsistent ones. This is based on mirror symmetry in the xz plane. The current in the y direction changes sign under this symmetry operation and thus vanishes.

The momentum-dependent contributions to the current in the half slab $0 \leq l < W/2$ are obtained by summing $\langle j_l \rangle$ over $l = 0, \dots, W/2 - 1$ and removing the factor $1/N_\parallel$ and the momentum sum. The momentum-resolved m component, which sums to a nonzero current, is shown in Fig. 5(c) in the main text. We present the momentum-resolved y and l components in Fig. S1. The y components cancel by symmetry, as noted above. The cancellation of the l components, which is required by charge conservation, is only ensured for selfconsistent gaps [S3]. Large positive contributions from bulk states within the projected (small) positive-helicity Fermi surface are canceled by small negative contributions from the flat bands and from bulk states within the projected (large) negative-helicity Fermi surface. This shows that the bulk states must be included to satisfy charge conservation.

[S1] A. P. Schnyder, P. M. R. Brydon, and C. Timm, Phys. Rev. B **85**, 024522 (2012).

[S2] W. H. Press, S. A. Teukolsky, W. T. Vetterling, and B. P. Flannery, *Numerical Recipes: The Art of Scientific Computing*, 3rd edition (Cambridge University Press, New York, 2007).

[S3] A. Furusaki and M. Tsukada, Solid State Commun. **78**, 299 (1991).

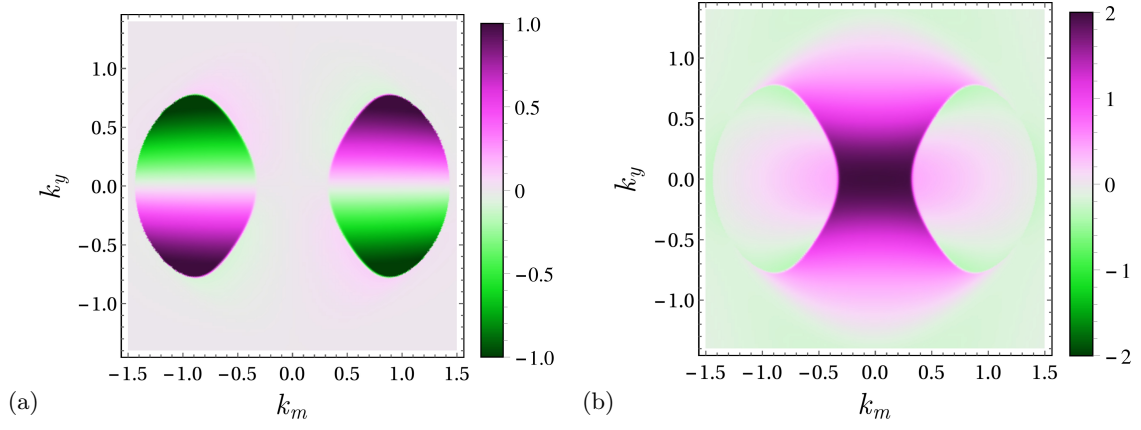


FIG. S1. Momentum-resolved contributions to (a) the y component and (b) the l component of the current in half the slab ($0 \leq l < W/2$).